

# The topological counterparts of non-Hermitian SSH models\*

Y. Z. Han, J. S. Liu, C. S. Liu

(Dated: March 24, 2021)

The breakdown of the conventional bulk-boundary correspondence due to non-Hermitian skin effect leads to the non-Bloch bulk-boundary correspondence in the generalized Brillouin zone. Inspired by the case of the equivalence between the non-reciprocal hopping and imaginary gauge field, we propose a method to construct the topological equivalent models of the non-Hermitian dimerized lattices with the similarity transformations. The idea of the constructions is from that the imaginary magnetic flux vanishes under the open boundary condition and the period boundary spectra can be well approximated by open boundary spectra. As an illustration, we apply this approach to several representative non-Hermitian SSH models, efficiently obtaining topological invariants in analytic form defined in the conventional Bloch bands. The method gives an alternative way to study the topological properties of non-Hermitian system.

## I. INTRODUCTION

The nonconservative phenomena existing widely in natural and artificial systems, e.g., open system coupled to energy or particle sources, or driven by external fields can be modeled by the effective non-Hermitian Hamiltonians [1–8]. The non-Hermitian systems have exhibited rich exotic characteristics without Hermitian counterparts [9–23]. The prominent character is the breakdown of the usual bulk-boundary correspondence in the nonreciprocal lattices due to the non-Hermitian skin effect [17–19, 24–33]. The non-Hermitian skin effect induces all the bulk states are localized at the boundaries of the system and are indistinguishable from the topological edge states. The novel topological invariants are needed to characterize topological properties. The pioneering research is the proposal of the generalized Brillouin zone (GBZ) which recovers the correspondence between the winding number based on complex energy with periodic boundaries and the existence of zero modes with open boundaries [24]. The calculation of GBZ becomes an important issue and has drawn extensive attentions recently [30, 34, 35].

It is well known that there is a Hermitian counterpart for a non-Hermitian Hamiltonian within the symmetry-unbroken region, in which the two Hamiltonians have an identical fully real spectrum [36–38]. This allows us to find the nontrivial states of the non-Hermitian Hamiltonian with the open boundary condition from its Hermitian counterpart. Here, a natural question that arises in this topics is whether there is a partner of non-Hermitian system with non-Hermitian skin effect that share the same topological phase diagrams. As such, the topological invariant of the original model can be obtained from its partner, which can be calculated in an easier way. In particular, the topological invariant of their partner may have the analytical form which is important to understand the whole properties of non-Hermitian system.

In general, the non-Hermitian skin effect comes from the non-reciprocal hopping of the lattice. This effect can be realized experimentally in atomic systems by laser assisted spin-selective dissipations [39, 40]. As the case studied in Ref. [14] and [17], the model with balanced hopping and only gains and

losses is mathematically equivalent to the non-Hermitian Su-Schrieffer-Heeger (SSH) model with the imbalance hopping when Pauli matrix  $\sigma_z$  is replaced by  $\sigma_y$ , although the original model can not be interpreted by SSH model. The recent study provides the conditions under which on-site dissipations can induce non-Hermitian skin modes [34].

The asymmetric couplings are equivalent to an imaginary gauge field applying to the lattice [10, 31]. Under the periodical boundary condition, the imaginary gauge field enclosed in an area induces a nonzero imaginary magnetic flux, which is non-Hermitian Aharonov-Bohm effect as the Hermitian case [31]. As pioneered by Yang and Lee in 1952, quantum phase transition can be driven by a complex external parameter [41, 42]. The nonzero imaginary magnetic flux breaks the conventional bulk-boundary correspondence and leads to a topological phase transition. Under the open boundary condition (OBC) however, the imaginary gauge field is not enclosed in an area and the imaginary magnetic flux vanishes [31]. Although the OBC breaks the translational symmetry, according to the bulk-boundary correspondence in the long chain case, the boundary scattering can still be regarded as a perturbation whether in Hermit case or not due to the introduction of the GBZ. This gives a strong hint that the Bloch Hamiltonian can be well approximated by the bulk Hamiltonian under the OBC. Following this route, non-Hermitian Bulk-boundary correspondence of the non-Hermitian SSH model without the  $t_3$  was recovered after getting rid of the effective imaginary gauge [31]. A key step is transforming the non-Hermitian terms to the Bloch phase factor with a similarity transformation. This step can also be realized under the OBC through another similarity transformation [24]. After the similarity transformation, the non-Hermitian SSH model is transformed to its topological equivalent model which leads to understand the nontrivial topological phase easily.

A natural issue is whether the method can be extended to construct the partner of the general non-Hermitian model with the asymmetric coupling terms. Motivated by the above considerations, we develop this method to construct the partners of several non-Hermitian SSH models. As is shown in the following studies, the central tenet of the constructing is building the relationship between non-Hermitian skin effect and imaginary equivalent gauge field. The topological invariants based on band-theory are effective to predict the topological nontrivial states. The remainder of this paper is organized

\* cslu@ysu.edu.cn

as follows. In Sec. II, we present the Hamiltonians of non-Hermitian SSH model and its various equivalent models. We show how the non-Hermitian SSH model is transformed to its equivalent models by the similarity transformations and how the non-Hermitian skin effect is eliminated due to the offset of the imaginary gauge field. In subsection III A, the effectively gauge field is found to construct a partner model of the non-Hermitian SSH model by a similarity transformation. Due to the topological equivalence of the two models, we study the topological phase transitions with the partner models in subsection III B. Inspired by the consistence of the QPTs with the numerical method, we further apply the method to study the non-Hermitian SSH model with spin-orbit coupling in Sec. IV A and the topological defect states of the non-Hermitian SSH model in Sec. IV B. Finally, a summary and discussion are given in Sec. V.

## II. THE NON-HERMITIAN SSH MODELS

The non-Hermitian SSH model is described Bloch Hamiltonian  $H_k = \psi_k^\dagger h_k \psi_k$  with  $h_k = (\vec{d} - i\vec{\Gamma}) \cdot \vec{\sigma}$ , where  $\vec{\sigma} = (\sigma_x, \sigma_y, \sigma_z)$  is the Pauli matrix for spin-1/2 and  $d_x = t_1 + (t_2 + t_3) \cos k$ ,  $d_y = (t_2 - t_3) \sin k$  [43, 44]. The Numb wavefunction  $\psi_k^\dagger = (a_k^\dagger, b_k^\dagger)$ . When Pauli matrix  $\sigma_y$  is replaced by  $\sigma_z$  and setting  $t_1 = M + 4B$ ,  $t_2 + t_3 = 2B$  and  $t_2 - t_3 = 2A$ , the generalized SSH model  $h_k$  can be mapped to 1D Creutz-type model [45] which is the dimensional reduced BHZ model [46, 47]. When Pauli matrix  $\sigma_x$  is replaced by  $\sigma_z$  and replacing  $t_1 = -\mu$ ,  $t_2 + t_3 = -2t$  and  $t_2 - t_3 = -2\Delta$ , the generalized SSH model  $h_k$  can be mapped to 1D Kitaev model [47, 48]. The non-Hermiticity comes from the term  $\vec{\Gamma}$ . When  $\vec{\Gamma} = (0, 0, \gamma/2)$ , the non-Hermiticity doesn't change the topological phase transition and the existence of the edge state due to the pseudo-anti-Hermiticity protection [19, 49, 50]. If the imaginary part  $\vec{\Gamma} = (\gamma/2, 0, 0)$ , the inversion symmetry of  $h_k$  ensures non-existence of the non-Hermitian skin effect and the validity of conventional bulk-boundary correspondence. The nontrivial topology is established from the linking geometry of the vector fields [44]. We study the case of  $\vec{\Gamma} = (0, \gamma/2, 0)$ . The non-Hermitian SSH model and its equivalent two-leg ladder model are pictorially shown in Fig. 1 (a) and (b). The Bloch Hamiltonian reads

$$h_k = d_x \sigma_x + (d_y + i\frac{\gamma}{2}) \sigma_y \quad (1)$$

where  $\sigma_{x,y}$  are the Pauli matrices. The asymmetric intracell coupling amplitude  $t_1 \pm \gamma/2$  can be realized in open classical and quantum systems with gain and loss [39, 40, 51, 52]. The model has a chiral symmetry  $\sigma_z^{-1} h_k \sigma_z = -h_k$ , which ensures that the eigenvalues appear in  $(E, -E)$  pairs.

There are various equivalent models for this model. For example, a mathematically equivalent model is studied in Ref. [11]. This model can be obtained by a similarity transformation  $\tilde{H} = S_1^{-1} H S_1$  with a diagonal matrix  $S_1$  whose diagonal elements are judiciously chosen as [24]

$$S_1 = \{1, r_1, r_1, r_1^2, r_1^2, \dots, r_1^{L/2-1}, r_1^{L/2-1}, r_1^L\} \quad (2)$$

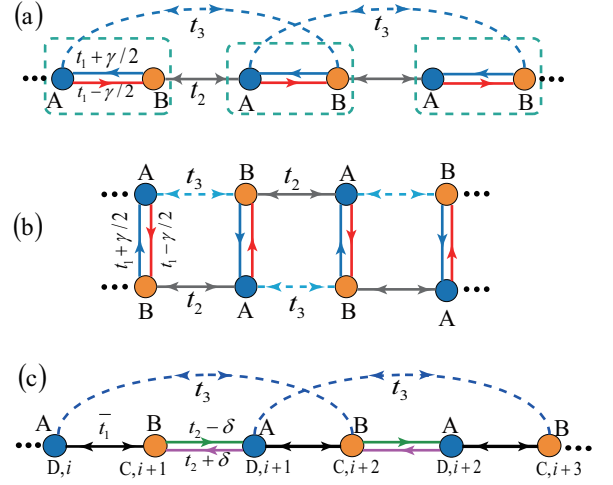


FIG. 1. (a) Non-Hermitian SSH model and (b) its equivalent two-leg ladder model. (c) Schematic of the mapping between the non-Hermitian SSH model in Eq. (1) and the extended non-Hermitian SSH model in Eq. (4).

here  $r_1 = \sqrt{|(t_1 - \gamma/2)/(t_1 + \gamma/2)|}$ . Under the similarity transformation, the non-Hermiticity in  $t_1$  term is transformed to  $t_3$  term where  $t_3$  term becomes  $t_3 r_1^2$  and  $t_3/r_1^2$ . The wavefunction  $|\psi\rangle = (a_1, b_1, a_2, b_2, \dots, a_L, b_L)^T$  becomes  $|\tilde{\psi}\rangle = S_1^{-1} |\psi\rangle$ . The intracell hopping  $\tilde{t}_1 = \sqrt{|t_1^2 - \gamma^2/4|}$  and the  $t_2$  term remains unchanged.

The extended non-Hermitian SSH discussed in Ref. [53] can be obtained by a similarity transformation  $\tilde{H} = S_2^{-1} \tilde{H} S_2$  with a diagonal matrix

$$S_2 = \text{diag}\{r_2, r_2, r_2^2, r_2^2, \dots, r_2^{L/2}, r_2^{L/2}\} \quad (3)$$

here  $r_2 = r_1^{-2}$ . After this transformation shown in Fig. 1 (c), the non-Hermiticity is transformed from  $t_3$  term to  $t_2$  term where  $t_2$  term becomes  $t_2/r_2$  and  $t_2 r_2$ . The wavefunction  $|\tilde{\tilde{\psi}}\rangle = S_2^{-1} |\tilde{\psi}\rangle$  and the intracell hopping  $\tilde{t}_1$  remains unchanged. By relabeling the sites  $A \rightarrow D$  and  $B \rightarrow C$ , the model can be mapped to an extended non-Hermitian SSH model. The Hamiltonian in momentum space takes the form

$$\tilde{H}_k = \sum_k \tilde{\psi}_k^\dagger \tilde{h}_k \tilde{\psi}_k,$$

where  $\tilde{\psi}_k = (c_k, d_k)^T$  and

$$\tilde{h}_k = \begin{pmatrix} 0 & t - \delta + t' e^{ik} + \Delta e^{-2ik} \\ t + \delta + t' e^{ik} + \Delta e^{2ik} & 0 \end{pmatrix}. \quad (4)$$

In the mapping, we have replaced  $\Delta = t_3$ ,  $t' = \tilde{t}_1$ ,  $t - \delta = t_2/r_2$  and  $t + \delta = t_2 r_2$ .

The non-Hermitian SSH model in Eq. (1) is also topological equivalence to the model discussed in Ref. [26] where the non-Hermiticity occurs in  $t_1$ ,  $t_2$  and  $t_3$  terms. One can first do the inverse similarity transformation in Eq. (3). The non-Hermiticity in  $t_2$  term is transferred to  $t_3$  term. Then further

doing the inverse similarity transformation in Eq. (2), the non-Hermiticity in  $t_3$  term is transferred to  $t_1$  term. After doing the two similarity transformations, the non-Hermiticity in  $t_2$  and  $t_3$  terms disappear and the asymmetric intercell coupling is transformed to symmetrical. The intercell coupling relating to  $t_1$  term remains asymmetrical.

### III. THE PARTNER MODEL AND TOPOLOGICAL INVARIANT

#### A. The partner model

The asymmetric couplings in  $t_1$  term of Eq. (1) can be expressed as a symmetric coupling  $\bar{t}_1$  with phase factor of amplification/attenuation  $e^{\pm\phi}$ , i.e.  $t_1 \pm \gamma/2 = \bar{t}_1 e^{\pm\phi}$ . Under the basis  $\psi_k' = \{e^{-\phi} a_k^\dagger, b_k^\dagger\} = \{a_k'^\dagger, b_k^\dagger\}$ , the Hamiltonian  $H_k$  can be rewritten in the form of

$$H_k = \psi_k'^\dagger \hat{h}_k \psi_k' = [\bar{t}_1 + t_2 e^\phi e^{-ik} + t_3 e^\phi e^{ik}] a_k'^\dagger b_k + [\bar{t}_1 + t_2 e^{-\phi} e^{ik} + t_3 e^{-\phi} e^{-ik}] b_k^\dagger a_k'. \quad (5)$$

With the similarity transformation, the AB sublattice becomes A'B sublattice and the asymmetric coupling is transformed from  $t_1$  term to  $t_2$  and  $t_3$  terms shown in Fig. 2 (a). Here, the site label A is replaced by A' which describes the annihilation operator  $a$  of A site is transformed to  $a'$ .

Assuming  $t_1, t_2, t_3$  and  $\phi$  to be greater than zero, the non-Hermitian skin effect in model (5) can be analysed in real space as follows. When  $t_2 \neq 0$  and  $t_3 = 0$  shown in 2 (b), the model (5) is reduced to the general non-Hermitian SSH model. The hopping  $t_2 e^\phi$  from B sites to A' sites is larger than that  $t_2 e^{-\phi}$  from A' to B sites. The asymmetry hopping leads to the particles tend to right side. However, in the case of  $t_3 \neq 0$  and  $t_2 = 0$  shown in 2 (c), the model (5) is also reduced to the general non-Hermitian SSH model where the hopping  $t_3 e^\phi$  from A' sites to B sites is larger than that  $t_3 e^{-\phi}$  from B to A' sites which induces the particles tend to left side. For the case  $t_2 = t_3 \neq 0$ , the Hamiltonian in Eq. (5) has the  $\mathcal{PT}$  symmetry and the two non-Hermitian skin effects cancel. Therefore, we conclude that there exist a non-Hermitian skin effect when  $t_2 \neq t_3$ . When  $t_2 > t_3$ , the non-Hermitian skin effect is governed by the  $t_2$  term and all the states are localized in the right edge. When  $t_2 < t_3$ ,  $t_3$  term dominates the non-Hermitian skin effect which leads the all the states localized in the right edge.

The amplification and attenuation factors  $e^{\pm\phi}$  in Eq. (5) indicate an imaginary gauge field  $\phi$  applying to the lattice. The effective imaginary gauge field can be analysed in moment space as follows. In the unit cell shown in Fig. 2 (d), two channels are provided for a particle tunneling from A' to B with different hopping amplitude. It indicates that a particle tunneling from A' site to B site will obtain a  $e^\phi$  phase for the  $t_2$  and  $t_3$  channels. The product of the above two terms contribute the overall accumulated phase factor  $e^{2\phi}$  which suggests the enclosed imaginary gauge field be  $2\phi$ .

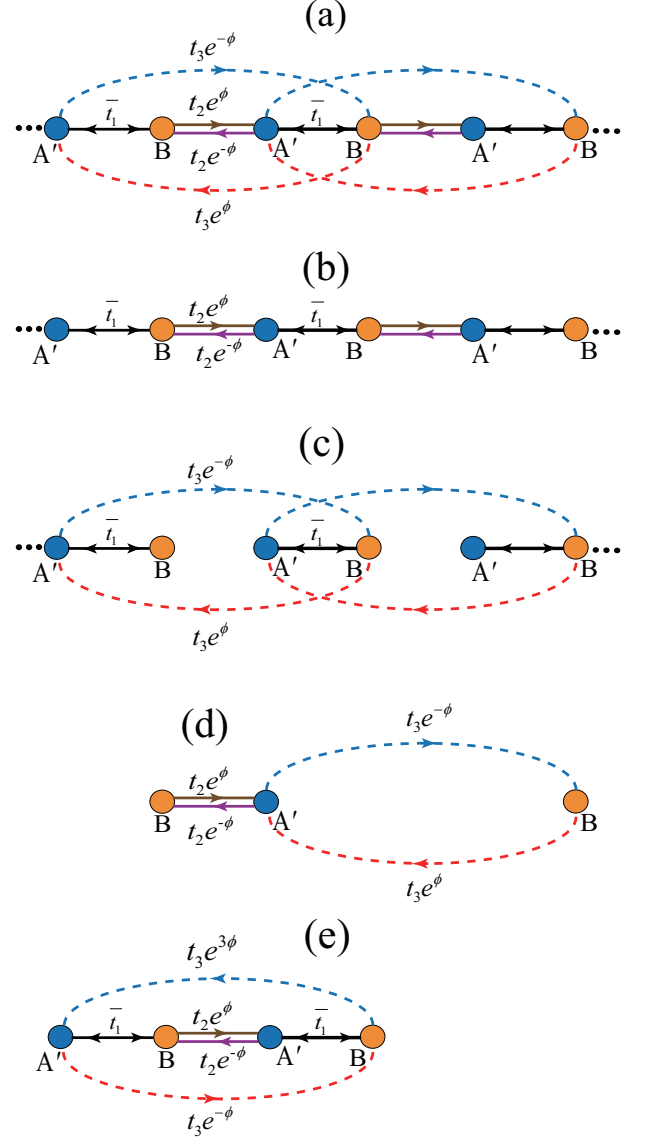


FIG. 2. (a) Schematic of the imaginary gauge field in Eq. (5) when  $t_2 \neq 0$  and  $t_3 \neq 0$ . Illustration of the non-Hermitian skin effect when (b)  $t_2 \neq 0, t_3 = 0$  and (c)  $t_2 = 0, t_3 \neq 0$ . (d) Illustration of the effective imaginary gauge field of the non-Hermitian SSH model in Eq. (5). (e) Illustration of the non-Hermitian skin effective of the partner model in Eq. (7).

We therefore rewrite  $\hat{h}_k$  in Eq. (5) as

$$\check{h}_k = [\bar{t}_1 + t_2 e^{-i(k+2i\phi)} e^{-\phi} + t_3 e^{i(k+2i\phi)} e^{3\phi}] \sigma_+ + [\bar{t}_1 + t_2 e^{i(k+2i\phi)} e^\phi + t_3 e^{-i(k+2i\phi)} e^{-3\phi}] \sigma_-, \quad (6)$$

where  $\sigma_\pm = \sigma_x \pm i\sigma_y$ . Considering the terms  $t_2 e^{-i(k+2i\phi)}$  and  $t_3 e^{i(k+2i\phi)}$  in Eq. (6), they are equivalent to an imaginary magnetic field applying to the A'B lattice. We take a complex-valued wave vector  $\tilde{k} \rightarrow k + 2i\phi$  to describe open-boundary eigenstates. In this replacement, the Hamiltonian (6) can be treated as parameter of  $\tilde{k}$  which a deformation of the standard

Brillouin zone. Accordingly, we define a partner Hamiltonian as follows:

$$\tilde{h}_{\tilde{k}} = h_+(\tilde{k})e^{i\theta_+(\tilde{k})}\sigma_+ + h_-(\tilde{k})e^{i\theta_-(\tilde{k})}\sigma_-, \quad (7)$$

which is also non-Hermitian Hamiltonian.  $h_+(\tilde{k})$  and  $\theta_+(\tilde{k})$  are the module and angle of complex function  $\tilde{t}_1 + t_2e^{-i\tilde{k}}e^{-\phi} + t_3e^{i\tilde{k}}e^{3\phi}$ .  $h_-(\tilde{k})$  and  $\theta_-(\tilde{k})$  are the module and angle of complex function  $\tilde{t}_1 + t_2e^{i\tilde{k}}e^{\phi} + t_3e^{-i\tilde{k}}e^{-3\phi}$ .

The partner model is still a non-Hermitian model. The non-Hermitian  $t_2$  and  $t_3$  terms lead to the accumulation of real phase factor which suggests the enclosed imaginary gauge field be  $2\phi$ . The  $2\phi$  imaginary gauge field suggests that the wave vector should be  $\tilde{k} \rightarrow \tilde{k} + 2i\phi$ . The model in Eq. (7) is transformed back to the model in Eq. (5).

The non-Hermitian skin effect in model (7) can also be analysed in real space. In the unit cell shown in Fig. 2(e),  $\pm\phi$  in the asymmetry hopping  $t_2$  term is equivalent to an imaginary magnetic field applied to the lattice with an imaginary magnetic vector potential  $i\phi$  alone  $x$  direction. For the asymmetry hopping  $t_3$  term,  $\pm 3\phi$  can be written as  $\pm\phi(3a)$  here the lattice constant  $a = 1$ .  $3a$  indicates three sites have been crossed when a particle hopping from B site to A' through the  $t_3$  channel. It is also equivalent to an imaginary magnetic field applied to the lattice with an imaginary magnetic vector potential  $i\phi$ . However, the imaginary magnetic vector potential is alone the  $-x$  direction. The two imaginary magnetic vector potentials are cancelled and the imaginary magnetic flux does not exist under the periodical boundary condition. No non-Hermitian skin effect occurs in the model [Eq. (6)] and wave vector is still a good quantum number.

The partner model in Eq. (7) is also effective to the case  $t_2 \neq 0$  and  $t_3 = 0$ . Replacing  $\tilde{k} \rightarrow \tilde{k} - i\phi$ , the partner model in Eq. (7) is transformed the standard SSH model with the phase transition point  $\tilde{t}_1 = t_2$ . When  $t_3 \neq 0$  and  $t_2 = 0$ , we can replace  $\tilde{k} \rightarrow \tilde{k} + 3i\phi$ . The partner model in Eq. (7) is also transformed the standard SSH model with the phase transition point  $\tilde{t}_1 = t_3$ . The above cases have been studied in Ref. [24] and [31].

Under the OBC, the partner Hamiltonian in Eq. (7) can also be obtained from the model in Eq. (1) by a similarity transformation  $\tilde{H} = S_3^{-1}HS_3$  directly.  $S_3 = S_1S_2$  is also a diagonal matrix where  $S_1$  and  $S_2$  are given in Eq. (2) and (3) with  $r_1 = r_2 = e^{\phi}$ . The similarity transformation changes the eigenstates and don't change its eigen-energy. So the models in Eq. (1) Eq. (5) and Eq. (7) are topological equivalent. As shown in Subsec. III B, the topological nontrivial phases can be characterized by the winding number based on the Eq. (7).

## B. The topological invariant

According to the usual bulk-boundary-correspondence scenario, the chiral edge states of an 1D open-boundary system should be determined by the winding numbers which are closely related to the Zak phase across the Brillouin zone [54]. For the non-Hermitian system with chiral symmetry and the

complex eigenvalues, the winding number of energy is defined as a topological invariant [15, 16, 49]. As  $\tilde{k}$  goes across the generalized Brillouin zone, the winding number of energy  $\nu_E$  is defined as

$$\nu_E = \frac{1}{2\pi} \oint d\tilde{k} [\partial_{\tilde{k}} \arg(E_2 - E_1)] \quad (8)$$

where the integral is also taken along a loop with  $\tilde{k}$  from 0 to  $2\pi$ . The eigenvalues of Hamiltonian (7) are

$$E_{1,2} = \pm \sqrt{h_+(\tilde{k})h_-(\tilde{k})} \exp\{i[\theta_+(\tilde{k}) + \theta_-(\tilde{k})]/2\}$$

which are smoothly continuous with  $\tilde{k}$ .  $\nu_E$  is summation of winding numbers of two winding vectors  $h_+(\tilde{k})e^{i\theta_+(\tilde{k})}$  and  $h_-(\tilde{k})e^{i\theta_-(\tilde{k})}$ . In Hermitian systems,  $\nu_E$  is always zero due to the real energy  $E_{1,2}$ .

The non-Bloch winding number can also be introduced with the “ $Q$  matrix” [19, 24, 29, 55]. The  $Q$  matrix is defined by

$$Q(\beta) = |\tilde{u}_R(\beta)\rangle\langle\tilde{u}_L(\beta)| - |u_R(\beta)\rangle\langle u_L(\beta)|,$$

where the right vector  $|u_R\rangle$  and left vector  $|u_L\rangle$  are defined by

$$\tilde{h}_{\tilde{k}}|u_R\rangle = E(\tilde{k})|u_R\rangle, \quad \tilde{h}_{\tilde{k}}^\dagger|u_L\rangle = E^*(\tilde{k})|u_L\rangle.$$

$|\tilde{u}_R\rangle \equiv \sigma_z|u_R\rangle$  and  $|\tilde{u}_L\rangle \equiv \sigma_z|u_L\rangle$  are also right and left eigenvectors, with eigenvalues  $-E$  and  $-E^*$  due to the chiral symmetry. The normalization conditions are  $\langle u_L|u_R\rangle = \langle \tilde{u}_L|\tilde{u}_R\rangle = 1$  and  $\langle u_L|\tilde{u}_R\rangle = \langle \tilde{u}_L|u_R\rangle = 0$ . The “ $Q$  matrix is off-diagonal, namely  $Q = q\sigma_+ + q^{-1}\sigma_-$  where  $q = \sqrt{h_2(\tilde{k})/h_1(\tilde{k})} \exp\{i[\theta_2(\tilde{k}) - \theta_1(\tilde{k})]/2\}$ . The non-Bloch winding number is given by

$$\nu_Q = \frac{i}{2\pi} \int_{C_B} q^{-1} dq \quad (9)$$

which is difference of winding numbers of two winding vectors  $h_+(\tilde{k})e^{i\theta_+(\tilde{k})}$  and  $h_-(\tilde{k})e^{i\theta_-(\tilde{k})}$ .

According to the geometry of two winding vectors  $h_+(\tilde{k})e^{i\theta_+(\tilde{k})}$  and  $h_-(\tilde{k})e^{i\theta_-(\tilde{k})}$ , at the phase transitions points, the quantum numbers must meet the relationship:

$$\begin{aligned} \tilde{t}_1 &= t_2e^{i\phi} + t_3e^{-3i\phi}, \\ \tilde{t}_1 &= t_2e^{-i\phi} + t_3e^{3i\phi}. \end{aligned} \quad (10)$$

Taking  $t_2 = 1$  and  $\gamma = 4/3$  for example, the phase transition points are  $t_1 = 1.5660$  and  $t_1 = 1.7050$  according to the Eq. (10). At  $t_1 = 1.5660$ , the system transforms firstly from topological nontrivial phase to topological trivial phase which is the result in Ref. [24].

To summarize the approach: With a similarity transformation, the non-Hermiticity of the model is transformed from  $t_1$  term to  $t_2$  and  $t_3$  terms. According to the non-Hermiticity of the equivalent model, the imaginary gauge field  $\Phi$  is obtained. Using the imaginary gauge field, the partner model is constructed with the Peierls replacement  $\tilde{k} \rightarrow k + i\Phi$ . At last, the non-Hermitian winding number is solved.

## IV. TWO APPLICATIONS

### A. The non-Hermitian SSH model with spin-orbit coupling

When spin-orbit coupling is taking into account, the non-Hermitian version of SSH model can be written by the Hamiltonian  $H = H_{\text{SSH}} + H_{\text{SOC}}$  [56] where

$$H_{\text{SSH}} = \sum_{n,\sigma} \left[ (t - \delta) a_{n,\sigma}^\dagger b_{n,\sigma} + (t + \delta) b_{n,\sigma}^\dagger a_{n,\sigma} + t' a_{n+1,\sigma}^\dagger b_{n,\sigma} + t' a_{n,\sigma}^\dagger b_{n+1,\sigma} \right],$$

where  $a_{n,\sigma}^\dagger$  ( $a_{n,\sigma}$ ) and  $b_{n,\sigma}^\dagger$  ( $b_{n,\sigma}$ ) are the electron creation (annihilation) operators with spin  $\sigma = (\uparrow \text{ or } \downarrow)$  on the sublattices A and B of the  $n$ th unit cell, respectively. The non-Hermiticity of the Hamiltonian is due to the introduction of  $\delta$ . The spin-orbit coupling Hamiltonian is described by

$$H_{\text{SOC}} = \sum_{n,\sigma} [\lambda a_{n,\sigma}^\dagger b_{n,-\sigma} - \lambda' a_{n,\sigma}^\dagger b_{n-1,-\sigma} + \text{h.c.}],$$

where  $\lambda$  and  $\lambda'$  denote the spin-orbit coupling amplitudes in the unit cell and between two adjacent unit cells, respectively. When the spin-orbit coupling is Dresshaus type, the coupling amplitudes  $\lambda$  and  $\lambda'$  are real value. Otherwise the coupling amplitudes are imaginary value when the spin-orbit coupling is Rashba type. Adopting periodic boundary conditions and Fourier transforming, the Hamiltonian  $H = H_{\text{SSH}} + H_{\text{SOC}}$  can be easily written as  $H = \sum_k \psi_k^\dagger h_k \psi_k$ , where  $\psi_k^\dagger = (a_{k,\uparrow}, b_{k,\uparrow}, a_{k,\downarrow}, b_{k,\downarrow})^\dagger$ , and

$$h_k = \begin{pmatrix} 0 & \zeta_k - \delta & 0 & \varsigma_k \\ \zeta_k^* + \delta & 0 & \varsigma_k^* & 0 \\ 0 & \varsigma_k & 0 & \zeta_k - \delta \\ \varsigma_k^* & 0 & \zeta_k^* + \delta & 0 \end{pmatrix}, \quad (11)$$

with  $\zeta_k = t + t' e^{-ik}$  and  $\varsigma_k = \lambda - \lambda' e^{-ik}$ .

The non-Hermitian skin effect of the model can be analysed as follow. When the spin-orbit coupling effect is negligible, the Hamiltonian in Eq. (11) is the direct-sum of two non-Hermitian SSH Hamiltonians. The non-Hermitian skin effect exists in the system. When the spin-orbit coupling effect dominates the system, the Hamiltonian (11) is a Hermitian. Therefore, the non-Hermitian skin effect exists in system. Considering the spin-up and spin-down of the particles, two channels have been provided for the particles tunneling from A sites to B sites of the AB sublattice. The spin-orbit coupling effect provides a new channel which induces the different spin particles tunneling from A sites to B sites.

Referring the non-Hermitian terms  $t_1 \pm \delta = \bar{t}_1 e^{\pm\phi}$ , the asymmetric hopping is equivalent to an imaginary magnetic field applying with the imaginary vector potential  $-i\phi$ . Considering the two channels, the effective imaginary field with vector potential  $-2i\phi$  is applying to the lattice. The  $-2i\phi$  vector potential suggests the wave vector should be with the Peierls replacement  $\vec{k} \rightarrow \vec{k} + 2i\phi$ .

To finish this replacement, we do the similarity transformation to the Hamiltonian in Eq. (11)  $\tilde{h}_k = S_4^{-1} h_k S_4$  with a diagonal matrix  $S$  whose diagonal elements are  $\{e^{-2\phi}, 1, e^{-2\phi}, 1\}$ .

After the similarity transformation, we obtain the partner model

$$\tilde{h}_k = \begin{pmatrix} 0 & \tilde{\zeta}_{k,+} & 0 & \varsigma_{k,+} \\ \tilde{\zeta}_{k,-} & 0 & \varsigma_{k,-} & 0 \\ 0 & \varsigma_{k,+} & 0 & \tilde{\zeta}_{k,+} \\ \varsigma_{k,-} & 0 & \tilde{\zeta}_{k,-} & 0 \end{pmatrix} \quad (12)$$

here  $\tilde{\zeta}_{k,\pm} = t e^{\pm\phi} + t' e^{\pm 2\phi} e^{\mp i k}$  and  $\tilde{\varsigma}_{k,\pm} = e^{\pm 2\phi} (\lambda - \lambda' e^{\mp i k})$ . The wave function becomes  $\psi_k^\dagger = (e^{2\phi} a_{k,\uparrow}, b_{k,\uparrow}, e^{2\phi} a_{k,\downarrow}, b_{k,\downarrow})^\dagger$ . The partner is still a non-Hermitian model. Under the OBC, the partner can be obtained by a similarity transformation  $\tilde{H} = S_1^{-1} H S_1$  with a diagonal matrix  $S_1$  given in Eq. (2), where  $r_1 = |(t_1 - \delta) / (t_1 + \delta)|$ . Under the similarity transformation, the non-Hermiticity is transformed to  $t$  and  $\lambda$  terms and the  $t_2$  term remains unchanged. The wavefunction  $|\psi\rangle = (a_1, b_1, a_2, b_2, \dots, a_L, b_L)^T$  becomes  $|\tilde{\psi}\rangle = S_1^{-1} |\psi\rangle$ .

For the non-Hermitian terms  $\lambda e^{\pm 2\phi}$ , the asymmetric hoppings are equivalent to an imaginary magnetic field applying to the sublattice with the imaginary vector potential  $2i\phi$ . Considering the spin-up and spin-down channels, the effective imaginary field with vector potential is  $-2i\phi$  applying the lattice. The effective imaginary fields are canceled. It indicates that the non-Hermitian skin effect disappears and the wave vector is a good quantum number in the partner model in Eq. (12).

The Hamiltonian  $\tilde{h}_k$  in Eq. (11) can be brought into the direct-sum of two block diagonal form by the unitary transformation

$$\hat{h}_k = U^\dagger \tilde{h}_k U = \hat{h}_{\text{up}} \oplus \hat{h}_{\text{down}} \quad (13)$$

here the two block matrixes are

$$\begin{aligned} \hat{h}_{\text{up}} &= (\tilde{\zeta}_{k,-} - \tilde{\varsigma}_{k,-}) \sigma_+ + (\tilde{\zeta}_{k,+} + \tilde{\varsigma}_{k,+}) \sigma_- \\ &= e^{-2\phi} (\eta_1^* + \delta) \sigma_+ + e^{2\phi} (\eta_1 - \delta) \sigma_-, \end{aligned} \quad (14)$$

$$\begin{aligned} \hat{h}_{\text{down}}(\vec{k}) &= (\tilde{\zeta}_{k,-} - \tilde{\varsigma}_{k,-}) \sigma_+ + (\tilde{\zeta}_{k,+} - \tilde{\varsigma}_{k,+}) \sigma_- \\ &= e^{-2\phi} (\eta_2^* + \delta) \sigma_+ + e^{2\phi} (\eta_2 - \delta) \sigma_-. \end{aligned} \quad (15)$$

here  $\eta_1 = \zeta_k + \varsigma_k$  and  $\eta_2 = \zeta_k - \varsigma_k$ . The unity matrix is

$$U = \frac{1}{\sqrt{2}} \begin{pmatrix} 0 & 1 & 0 & 1 \\ 1 & 0 & 1 & 0 \\ 0 & 1 & 0 & -1 \\ 1 & 0 & -1 & 0 \end{pmatrix}.$$

$\hat{h}_{\text{up}}$  and  $\hat{h}_{\text{down}}$  show chiral symmetry defined respectively as  $C \hat{h}_{\text{up(down)}} C^{-1} = -\hat{h}_{\text{up(down)}}$ , where  $C = \sigma_z$ . The topological invariants of the non-Hermitian systems in Eq. (14) and (15) are the winding numbers of energy defined in Eq. (8). The winding number  $\hat{h}_{\text{up}}$  in Eq. (14) is just the summation of the winding numbers of the two vectors  $(\eta_1 - \delta)$ ,  $-(\eta_1^* + \delta)$ . The winding number  $\hat{h}_{\text{down}}$  in Eq. (15) is the summation of the winding numbers of the two vectors  $(\eta_2 - \delta)$ ,  $-(\eta_2^* + \delta)$ . The results have obtained and confirmed numerically in Ref. [56].

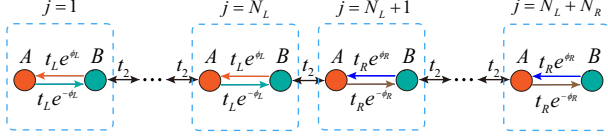


FIG. 3. Schematic of a non-Hermitian SSH model under the domain-wall configuration. The intra-cell hopping from sublattice sites  $a$  to  $b$  in the left(right) bulk is  $t_L^{(R)} e^{\phi_{L(R)}}$ , while the intra-cell hopping from  $b$  to  $a$  is  $t_L^{(L(R))} e^{-\phi_{L(R)}}$ . For simplicity, we assume both bulks have the same  $t_2$ .

### B. The topological defect on non-Hermitian SSH model

The above method can also be applied to other model. For example, the topological defect on non-Hermitian SSH model. The defect is an useful tool to probe the nontrivial topological properties of bulk systems [57–60]. The topological defect on non-Hermitian lattices with spatially distributed gain and loss was discussed [61–63]. Two bulks with topologically distinct phases contacting through a common boundary form a domain wall configuration is a special topological defect where the domain wall state is exponentially localized at the interface between two different bulks. Recently, some non-Hermitian topological systems in domain wall configuration were studied theoretically and experimentally [51, 52, 63–65].

A non-Hermitian SSH model in a domain-wall configuration on a ring has been investigated numerically in Ref. [65]. When the length of the two chains is large, the domain can be taken as a perturbation. In particular, the coupling of the domain states can also be neglected. The energy spectra of the domain-wall configuration on the ring can be well approximated by that on a chain. A non-Hermitian SSH model in a domain-wall configuration on a chain is pictorially shown in Fig. 3. The Hamiltonian can be written as

$$H = H_L + H_R, \quad (16)$$

where

$$H_\alpha = \sum_j \left[ t_\alpha e^{i\phi_\alpha} a_j^\dagger b_j + t_\alpha e^{-i\phi_\alpha} b_j^\dagger a_j + t_2 a_{j+1}^\dagger b_j + t_2 b_j^\dagger a_{j+1} \right],$$

here  $\alpha = (L, R)$  denotes the left or right bulk.  $a_j^\dagger$  ( $a_j$ ) and  $b_j^\dagger$  ( $b_j$ ) are the creation (annihilation) operators for the sublattice sites  $a$  and  $b$  on the  $j$ -th unit cell. The left and right bulks have different parameters and contain  $N_L$  and  $N_R$  unit cells respectively. The non-Hermiticity of the system is from the difference intra-cell hopping with phase factor of amplification/attenuation  $e^{\pm\phi_\alpha}$ . The non-Hermitian SSH model has also chiral symmetry  $\Gamma H \Gamma^{-1} = -H$ , with the chiral-symmetry operator  $\Gamma = \sum_{j=1}^{N_L+N_R} (a_j^\dagger a_j - b_j^\dagger b_j)$ .

To understand the topological properties of the model, we do the following transformation to the Hamiltonian in Eq.

(16):

$$H = \langle \Psi | h | \Psi \rangle = \langle \Phi | \bar{h} | \Phi \rangle,$$

here  $\bar{h} = S^{-1} h S$  and

$$|\psi\rangle = (a_1, b_1, \dots, a_{N_L}, b_{N_L}, \dots, a_{N_L+N_R}, b_{N_L+N_R})^T$$

and

$$|\Phi\rangle = S |\psi\rangle = (c_1, d_1, \dots, c_{N_L}, d_{N_L}, \dots, c_{N_L+N_R}, d_{N_L+N_R})^T.$$

The transformation matrix  $S = S_1 S_2$ .  $S_1$  and  $S_2$  are the diagonal matrices. The diagonal elements of  $S_1$  are seted as

$$\{1, r, r, r^2, r^2, \dots, r^{N_L-1}, r^{N_L-1}, r^{N_L}, r^{N_R}, r^{N_R-1}, r^{N_R-1}, \dots, r^2, r^2, r, r, 1\}$$

with  $r = e^{(\phi_R - \phi_L)/2}$ . After the similarity transformation  $S_1$ , we have the same amplification/attenuation  $e^{\pm\phi}$  of phase factor in asymmetric couplings of the two bulks, here  $\phi = (\phi_R + \phi_L)/2$ . Then further doing the similarity transformation  $S_2$  with a diagonal matrix whose diagonal elements are selected as

$$(1, r, r, r^2, r^2, \dots, r^{N_L}, r^{N_L}, \dots, r^{N_L+N_R-1}, r^{N_L+N_R-1}, r^{N_L+N_R}),$$

we get the Hermitian Hamiltonian of the two bulks connecting in a chain configuration

$$H_\alpha = \sum_j (t_\alpha c_j^\dagger d_j + t_\alpha d_j^\dagger c_j + t_2 c_{j+1}^\dagger d_j + h.c.).$$

When the two bulks connecting in a ring, we get the partner model of non-Hermitian SSH model in domain configuration studied in Ref.[65]. The Bloch winding number of this model is the winding number different  $\nu_R - \nu_L$  of the two bulks. The transition points of the two bulks are  $t_L = t_2$  and  $t_R = t_2$ .

Another type of defect is impurity which can vary the forward and backward scattering amplitude of the continuous states and induce gap bound states. The gap bound states are exponentially localized at the impurity [66, 67]. A hard-wall boundary is a special impurity which is equivalent to the infinity impurity strength and the forward scattering is forbidden. The single-impurity problem in the non-Hermitian SSH model is shown in Ref. [68].

According to bulk-boundary correspondence, when the lattice is long enough, the impurity state on the dimer ring can be approximated by that on the long chain since the boundary scattering can be regarded as a perturbation. The Hamiltonian of impurity problem is described by

$$H_{ip} = H_{SSH} + v a_0^\dagger a_0 = \psi^\dagger h_{ip} \psi, \quad (17)$$

where  $v$  is the strength of the impurity potential and  $\psi^\dagger = (a_{-L/2}^\dagger, b_{-L/2}^\dagger, a_{-L/2+1}^\dagger, b_{-L/2+1}^\dagger, \dots, a_{L/2}^\dagger, b_{L/2}^\dagger)$  with lattice length  $L$ . The non-Hermitian SSH Hamiltonian

$$H_{SSH} = \sum_{j=-L/2}^{L/2} (t e^{\phi} a_j^\dagger b_j + t e^{-\phi} b_j^\dagger a_j + t' a_{j+1}^\dagger b_j + t' b_{j+1}^\dagger a_j).$$

Here  $te^{\pm\phi}$  is the right (left) intra-hopping amplitude and  $t'$  is the inter-hopping amplitude.

The partner of the impurity model can be obtained by a conventional similarity transformation  $\tilde{h}_{ip} = S^{-1}h_{ip}S$  with a diagonal matrix

$$S = \text{diag}\{1, r, r, r^2, r^2, \dots, r^{L/2}, r^{L/2}\},$$

here  $r = e^{\phi}$ . After this transformation,  $H_{SSH}$  becomes the standard SSH model with the intra-hopping amplitude and the inter-hopping amplitude  $t'$ . The wavefunction  $|\tilde{\psi}\rangle = S^{-1}|\psi\rangle$  and the strength of the impurity potential  $v$  remains unchanged. The transition points are  $t = t'$ .

## V. SUMMARY

In summary, we have proposed a way to construct a counterpart of non-Hermitian SSH model. The kernel of this method is to find the effectively imaginary gauge field referring to the non-Hermitian skin effect under PBC. Under the OBC, the imaginary magnetic flux vanishes and the OBC spectra is used to approximate the PBC spectra. The corre-

sponding Hamiltonian is the counterpart of the original model. In fact, the partner model can be obtained by a similarity transformation. Due to the skin effect is eliminated from the wave vector, we can study the topological equivalent model in conventional Bloch space. Our work gives an alternating method to study the non-Hermitian SSH model with its counterpart. Several non-Hermitian SSH models are used to illustrate the method and phase transition points are given in analytic form. This method is expected to be used to construct the counterpart of a class of non-Hermitian model. In view of the non-reciprocal hopping, the similarity transformations and the effective imaginary gauge fields may depend on model details without any general rules. Not all of the non-Hermitian models may have the partner models constructed by this method, for example, the models proposed in Refs. [30, 32, 34]. Finding their counterparts is still a challenging subject.

## ACKNOWLEDGMENTS

This work was supported by Hebei Provincial Natural Science Foundation of China (Grant No. A2012203174, No. A2015203387) and National Natural Science Foundation of China (Grant No. 10974169, No. 11304270).

- 
- [1] Ingrid Rotter, “A non-hermitian hamilton operator and the physics of open quantum systems,” *Journal of Physics A: Mathematical and Theoretical* **42**, 153001 (2009).
  - [2] E. Persson, I. Rotter, H.-J. Stöckmann, and M. Barth, “Observation of resonance trapping in an open microwave cavity,” *Phys. Rev. Lett.* **85**, 2478–2481 (2000).
  - [3] Carl M Bender, “Making sense of non-hermitian hamiltonians,” *Reports on Progress in Physics* **70**, 947–1018 (2007).
  - [4] Y Choi, S. Kang, S Lim, W Kim, J. R. Kim, J. H. Lee, and K. An, “Quasieigenstate coalescence in an atom-cavity quantum composite,” *Phys. Rev. Lett.* **104**, 153601 (2010).
  - [5] N. Moiseyev, *Non-Hermitian Quantum Mechanics* (Cambridge University Press, Cambridge, 2011).
  - [6] Florentin Reiter and Anders S. Sørensen, “Effective operator formalism for open quantum systems,” *Phys. Rev. A* **85**, 032111 (2012).
  - [7] Ling Lu, John D. Joannopoulos, and Marin Soljačić, “Topological photonics,” *Nature Photonics* **8**, 821–829 (2014).
  - [8] I Rotter and J P Bird, “A review of progress in the physics of open quantum systems: theory and experiment,” *Reports on Progress in Physics* **78**, 114001 (2015).
  - [9] Naomichi Hatano and David R. Nelson, “Vortex pinning and non-hermitian quantum mechanics,” *Phys. Rev. B* **56**, 8651–8673 (1997).
  - [10] Naomichi Hatano and David R. Nelson, “Localization transitions in non-hermitian quantum mechanics,” *Phys. Rev. Lett.* **77**, 570–573 (1996).
  - [11] Kenta Esaki, Masatoshi Sato, Kazuki Hasebe, and Mahito Kohmoto, “Edge states and topological phases in non-hermitian systems,” *Phys. Rev. B* **84**, 205128 (2011).
  - [12] Baogang Zhu, Rong Lü, and Shu Chen, “ $\mathcal{PT}$  symmetry in the non-hermitian su-schrieffer-heeger model with complex boundary potentials,” *Phys. Rev. A* **89**, 062102 (2014).
  - [13] C. Yuce, “Topological phase in a non-hermitian pt symmetric system,” *Physics Letters A* **379**, 1213 – 1218 (2015).
  - [14] Tony E. Lee, “Anomalous edge state in a non-hermitian lattice,” *Phys. Rev. Lett.* **116**, 133903 (2016).
  - [15] Daniel Leykam, Konstantin Y. Bliokh, Chunli Huang, Y. D. Chong, and Franco Nori, “Edge modes, degeneracies, and topological numbers in non-hermitian systems,” *Phys. Rev. Lett.* **118**, 040401 (2017).
  - [16] Huitao Shen, Bo Zhen, and Liang Fu, “Topological band theory for non-hermitian hamiltonians,” *Phys. Rev. Lett.* **120**, 146402 (2018).
  - [17] V. M. Martinez Alvarez, J. E. Barrios Vargas, and L. E. F. Foa Torres, “Non-hermitian robust edge states in one dimension: Anomalous localization and eigenspace condensation at exceptional points,” *Phys. Rev. B* **97**, 121401 (2018).
  - [18] Ye Xiong, “Why does bulk boundary correspondence fail in some non-hermitian topological models,” *Journal of Physics Communications* **2**, 035043 (2018).
  - [19] Flore K. Kunst, Elisabet Edvardsson, Jan Carl Budich, and Emil J. Bergholtz, “Biorthogonal bulk-boundary correspondence in non-hermitian systems,” *Phys. Rev. Lett.* **121**, 026808 (2018).
  - [20] Zongping Gong, Yuto Ashida, Kohei Kawabata, Kazuaki Takasan, Sho Higashikawa, and Masahito Ueda, “Topological phases of non-hermitian systems,” *Phys. Rev. X* **8**, 031079 (2018).
  - [21] Chun-Hui Liu, Hui Jiang, and Shu Chen, “Topological classification of non-hermitian systems with reflection symmetry,” *Phys. Rev. B* **99**, 125103 (2019).
  - [22] Kohei Kawabata, Ken Shiozaki, Masahito Ueda, and Masatoshi Sato, “Symmetry and topology in non-hermitian physics,” *Phys. Rev. X* **9**, 041015 (2019).



- [23] Kohei Kawabata, Takumi Bessho, and Masatoshi Sato, “Classification of exceptional points and non-hermitian topological semimetals,” *Phys. Rev. Lett.* **123**, 066405 (2019).
- [24] Shunyu Yao and Zhong Wang, “Edge states and topological invariants of non-hermitian systems,” *Phys. Rev. Lett.* **121**, 086803 (2018).
- [25] Shunyu Yao, Fei Song, and Zhong Wang, “Non-hermitian chern bands,” *Phys. Rev. Lett.* **121**, 136802 (2018).
- [26] Kazuki Yokomizo and Shuichi Murakami, “Non-bloch band theory of non-hermitian systems,” *Phys. Rev. Lett.* **123**, 066404 (2019).
- [27] Fei Song, Shunyu Yao, and Zhong Wang, “Non-hermitian skin effect and chiral damping in open quantum systems,” *Phys. Rev. Lett.* **123**, 170401 (2019).
- [28] Ching Hua Lee and Ronny Thomale, “Anatomy of skin modes and topology in non-hermitian systems,” *Phys. Rev. B* **99**, 201103 (2019).
- [29] Fei Song, Shunyu Yao, and Zhong Wang, “Non-hermitian topological invariants in real space,” *Phys. Rev. Lett.* **123**, 246801 (2019).
- [30] Kai Zhang, Zhesen Yang, and Chen Fang, “Correspondence between winding numbers and skin modes in non-hermitian systems,” *Phys. Rev. Lett.* **125**, 126402 (2020).
- [31] L. Jin and Z. Song, “Bulk-boundary correspondence in a non-hermitian system in one dimension with chiral inversion symmetry,” *Phys. Rev. B* **99**, 081103 (2019).
- [32] Qi-Bo Zeng, Yan-Bin Yang, and Yong Xu, “Topological phases in non-hermitian aubry-andré-harper models,” *Phys. Rev. B* **101**, 020201 (2020).
- [33] Ching Hua Lee, Linhu Li, Ronny Thomale, and Jiangbin Gong, “Unraveling non-hermitian pumping: Emergent spectral singularities and anomalous responses,” *Phys. Rev. B* **102**, 085151 (2020).
- [34] Yifei Yi and Zhesen Yang, “Non-hermitian skin modes induced by on-site dissipations and chiral tunneling effect,” *Phys. Rev. Lett.* **125**, 186802 (2020).
- [35] Zhesen Yang, Kai Zhang, Chen Fang, and Jiangping Hu, “Non-hermitian bulk-boundary correspondence and auxiliary generalized brillouin zone theory,” *Phys. Rev. Lett.* **125**, 226402 (2020).
- [36] Carl M. Bender and Stefan Boettcher, “Real spectra in non-hermitian hamiltonians having  $\mathcal{PT}$  symmetry,” *Phys. Rev. Lett.* **80**, 5243–5246 (1998).
- [37] Ali Mostafazadeh, “Pseudo-hermiticity versus  $\mathcal{PT}$  symmetry: The necessary condition for the reality of the spectrum of a non-hermitian hamiltonian,” *Journal of Mathematical Physics* **43**, 205–214 (2002), <https://doi.org/10.1063/1.1418246>.
- [38] C. Li, X. Z. Zhang, G. Zhang, and Z. Song, “Topological phases in a kitaev chain with imbalanced pairing,” *Phys. Rev. B* **97**, 115436 (2018).
- [39] Samantha Lapp, Jackson Ang’ong’a, Fangzhao Alex An, and Bryce Gadway, “Engineering tunable local loss in a synthetic lattice of momentum states,” *New Journal of Physics* **21**, 045006 (2019).
- [40] Jiaming Li, Andrew K. Harter, Ji Liu, Leonardo de Melo, Yogesh N. Joglekar, and Le Luo, “Observation of parity time symmetry breaking transitions in a dissipative floquet system of ultracold atoms,” *Nat. Commun.* **855**, 1 (2019).
- [41] C. N. Yang and T. D. Lee, “Statistical theory of equations of state and phase transitions. i. theory of condensation,” *Phys. Rev.* **87**, 404–409 (1952).
- [42] T. D. Lee and C. N. Yang, “Statistical theory of equations of state and phase transitions. ii. lattice gas and ising model,” *Phys. Rev.* **87**, 410–419 (1952).
- [43] W. P. Su, J. R. Schrieffer, and A. J. Heeger, “Solitons in polyacetylene,” *Phys. Rev. Lett.* **42**, 1698–1701 (1979).
- [44] H. C. Wu, X. M. Yang, L. Jin, and Z. Song, “Untying links through anti-parity-time-symmetric coupling,” *Phys. Rev. B* **102**, 161101 (2020).
- [45] Michael Creutz, “End states, ladder compounds, and domain-wall fermions,” *Phys. Rev. Lett.* **83**, 2636–2639 (1999).
- [46] B. A. Bernevig, T. L. Hughes, and S.-C. Zhang, “Quantum spin hall effect and topological phase transition in hgte quantum wells,” *Science* **314**, 1757–1761 (2006).
- [47] Huai-Ming Guo, “A brief review on one-dimensional topological insulators and superconductors,” *Science China Physics, Mechanics & Astronomy* **59**, 637401 (2016).
- [48] A Yu Kitaev, “Unpaired majorana fermions in quantum wires,” *Physics-Uspekhi* **44**, 131–136 (2001).
- [49] Hui Jiang, Chao Yang, and Shu Chen, “Topological invariants and phase diagrams for one-dimensional two-band non-hermitian systems without chiral symmetry,” *Phys. Rev. A* **98**, 052116 (2018).
- [50] K. L. Zhang, H. C. Wu, L. Jin, and Z. Song, “Topological phase transition independent of system non-hermiticity,” *Phys. Rev. B* **100**, 045141 (2019).
- [51] Lei Xiao, Tianshu Deng, Kunkun Wang, Gaoyan Zhu, Zhong Wang, Wei Yi, and Peng Xue, “Non-Hermitian bulk-boundary correspondence in quantum dynamics,” *Nature Physics* **16**, 761–766 (2020).
- [52] T. Helbig, T. Hofmann, S. Imhof, M. Abdelghany, T. Kiessling, L. W. Molenkamp, C. H. Lee, A. Szameit, M. Greiter, and R. Thomale, “Generalized bulk-boundary correspondence in non-Hermitian topoelectrical circuits,” *Nature Physics* **16**, 747–750 (2020).
- [53] Chuanhao Yin, Hui Jiang, Linhu Li, Rong Lü, and Shu Chen, “Geometrical meaning of winding number and its characterization of topological phases in one-dimensional chiral non-hermitian systems,” *Phys. Rev. A* **97**, 052115 (2018).
- [54] J. Zak, “Berry’s phase for energy bands in solids,” *Phys. Rev. Lett.* **62**, 2747–2750 (1989).
- [55] Ching-Kai Chiu, Jeffrey C. Y. Teo, Andreas P. Schnyder, and Shinsei Ryu, “Classification of topological quantum matter with symmetries,” *Rev. Mod. Phys.* **88**, 035005 (2016).
- [56] Y.Z. Han, H. Jiang, Shu Chen, and C. S. Liu, “The nontrivial topological phases of a one-dimensional non-hermitian dimerized lattice with spin-orbit coupling and zeeman field,” *Physica E: Low-dimensional Systems and Nanostructures* **110**, 68–73 (2019).
- [57] Jeffrey C. Y. Teo and C. L. Kane, “Topological defects and gapless modes in insulators and superconductors,” *Phys. Rev. B* **82**, 115120 (2010).
- [58] Lukas Kimme and Timo Hyart, “Existence of zero-energy impurity states in different classes of topological insulators and superconductors and their relation to topological phase transitions,” *Phys. Rev. B* **93**, 035134 (2016).
- [59] Jie Lu, Wen-Yu Shan, Hai-Zhou Lu, and Shun-Qing Shen, “Non-magnetic impurities and in-gap bound states in topological insulators,” *New Journal of Physics* **13**, 103016 (2011).
- [60] Li-Jun Lang and Shu Chen, “Topologically protected mid-gap states induced by impurity in one-dimensional superlattices,” *Journal of Physics B: Atomic, Molecular and Optical Physics* **47**, 065302 (2014).
- [61] C. Yuce, “Edge states at the interface of non-hermitian systems,” *Phys. Rev. A* **97**, 042118 (2018).
- [62] Ya-Jie Wu and Junpeng Hou, “Symmetry-protected localized states at defects in non-hermitian systems,” *Phys. Rev. A* **99**, 062107 (2019).



- [63] Li-Jun Lang, You Wang, Hailong Wang, and Y. D. Chong, “Effects of non-hermiticity on su-schrieffer-heeger defect states,” *Phys. Rev. B* **98**, 094307 (2018).
- [64] Simon Malzard, Charles Poli, and Henning Schomerus, “Topologically protected defect states in open photonic systems with non-hermitian charge-conjugation and parity-time symmetry,” *Phys. Rev. Lett.* **115**, 200402 (2015).
- [65] Tian-Shu Deng and Wei Yi, “Non-bloch topological invariants in a non-hermitian domain wall system,” *Phys. Rev. B* **100**, 035102 (2019).
- [66] Henning Schomerus, “Topologically protected midgap states in complex photonic lattices,” *Opt. Lett.* **38**, 1912–1914 (2013).
- [67] Stefano Longhi, “Bound states in the continuum in pt-symmetric optical lattices,” *Opt. Lett.* **39**, 1697–1700 (2014).
- [68] Yanxia Liu and Shu Chen, “Diagnosis of bulk phase diagram of nonreciprocal topological lattices by impurity modes,” *Phys. Rev. B* **102**, 075404 (2020).